Journal of Alloys and Compounds 509 (2011) 6621–6625

Contents lists available at ScienceDirect

Journal of Alloys and Compounds

journal homepage: www.elsevier.com/locate/jallcom

Crystallization and magnetic behavior of nanosized nickel ferrite prepared by citrate precursor method

Dao Thi Thuy Nguyet [a], Nguyen Phuc Duong [a,*], Le Thanh Hung [a], Than Duc Hien [a], Takuya Satoh [b,c]

[a] International Training Institute for Materials Science (ITIMS), Hanoi University of Technology, 1 Dai Co Viet Road, Hanoi, Viet Nam
[b] Institute of Industrial Science, The University of Tokyo, Komaba, Meguro-ku, Tokyo 153-8505, Japan
[c] PRESTO, Japan Science and Technology Agency, Kawaguchi, Saitama 332-0012, Japan

ARTICLE INFO

Article history:
Received 17 November 2010
Accepted 18 March 2011
Available online 27 March 2011

Keywords:
Nickel ferrite
Nanoparticles
Citrate sol–gel
Curie temperature
Magnetization
Coercivity

ABSTRACT

$NiFe_2O_4$ nanoparticles have been synthesized by citrate precursor gel formation with subsequent heat treatment. Differential thermal and thermogravimetric (DTA/TG) analyses show that the metal citrates decomposed around 230 °C followed by crystallization of the ferrite. X-ray diffraction (XRD) patterns reveal the formation of the cubic spinel phase in the samples after sintering the gel at 350 °C, 500 °C and 700 °C. For the samples annealed at 350 °C and 500 °C a small amount of α-Fe_2O_3 was detected whereas single phase was obtained for the sample annealed at 700 °C. The lattice constant a for all the samples is comparable to the value of the bulk material. The mean crystallite size D_{XRD} of the samples determined from XRD line broadening is 26.2–28.5 nm. Transmission electron microscope (TEM) analysis shows that the single-phase particles form clusters with the particle size in the range of 21–82.5 nm and the most probable value D_{TEM} of 55.4 nm. Magnetic measurements show that its Curie temperature T_C is close to the bulk value while the spontaneous magnetization M_s at 5 K is lower than that of the bulk. The thermal variation of M_s in the temperature range from 5 to 300 K can be best fitted to a modified Bloch T^α law with the exponent value $\alpha \approx 2$. The magnetization data are explained with reference to the disordered surface spins and the finite size effects. In this investigated temperature range, the coercive force H_c decreases linearly with increasing temperature. The coercivity mechanism in the nanoparticle sample with broad particle size distribution is expected to be complex and different factors which affect the H_c value were proposed.

1. Introduction

Nickel ferrite is a typical inverse spinel structure where Fe^{3+} ions are located in the tetrahedral (A) and octahedral (B) sites and Ni^{2+} ions are located in octahedral sites only. The magnetic moments of the tetrahedral and octahedral sublattices couple antiparallelly and form a collinear ferrimagnetic ordering (Néel type) with the Curie temperature of about 870 K [1]. This compound has been widely used in electronic devices due to their large permeability at high frequency, high electrical resistivity and mechanical hardness [2,3]. Modern applications of magnetic nanoparticles in magneto-optical devices, contrasting agents in magnetic resonance imaging, magnetic refrigeration and ferrofluid technology have renewed the interest in the ferrite compounds in nanocrystalline forms [4–6]. The properties of these systems are known to be very sensitive to the physical factors such as the size, shape, and surface properties of the particles, the composition and purity of the system and the interactions among the particles. In this context, considerable attention has been paid on the magnetism and its related phenomena in the nickel ferrite nanoparticles including superparamagnetism, surface and finite size effects [7–9]. These nanoparticles possess a large surface to volume ratio, as a result of which the surface spins play a dominant role in defining the magnetic properties of the system. The spatial confinement at nanoscale implies that the role of surface atoms, with reduced symmetry, is enhanced and the consequent larger number of broken exchange bonds can result in surface anisotropy, frustration and spin disorder [9]. The surface spins cause the reduction of saturation magnetization with decreasing size and enhancement of coercivity and magnetic relaxation effects in these nanoparticles [9]. Such particles are generally termed as the core–shell nanoparticles, where the core spins behave like ferrimagnetic and the shell is composed of disordered spins or canted spins. The variation of the saturation magnetization at low temperature range also account for the finite size effect and surface contribution which is manifested via modified Bloch law's behavior for spin waves [10]. In order to tailor the size, morphology and magnetic properties of the nickel ferrite nanoparticles different preparation techniques have

* Corresponding author. Tel.: +84 4 38680787; fax: +84 4 38692963.
E-mail address: duong@itims.edu.vn (N.P. Duong).

0925-8388/$ – see front matter © 2011 Elsevier B.V. All rights reserved.
doi:10.1016/j.jallcom.2011.03.112

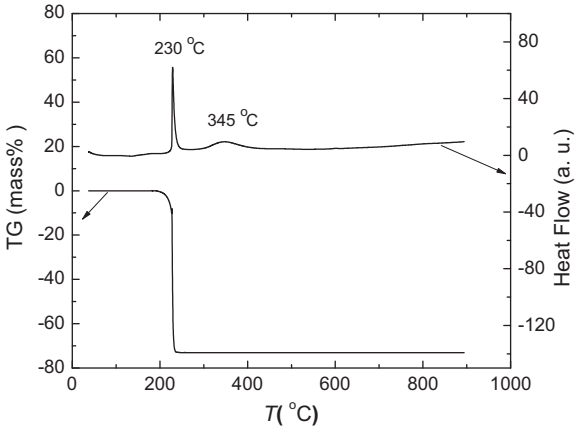

Fig. 1. DTA/TG thermogram of the citrate gel.

been used such as sol–gel [11], reverse micelle [7], aerosol [12], co-precipitation [10] and mechanical milling [9].

In this paper, the preparation of nickel ferrite nanoparticles by a citrate precursor gel formation route at moderate temperatures and its characterization by DTA/TG, XRD, TEM and magnetic measurements are presented.

2. Experiment

Amounts of $Ni(NO_3)_2$ and $Fe(NO_3)_3$ with molar ratio $[Ni^{2+}]/[Fe^{3+}] = 1/2$ were dissolved completely in deionized water. The aqueous solution containing Ni^{2+} and Fe^{3+} was poured into citric acid with the total cations/citric acid molar ratio = 1/1. Ammonium hydroxide in aqueous form was added to the mixed solutions and the pH of the solutions was adjusted to about 7. The mixtures were stirred at 600 rpm and slowly evaporated at 80 °C to form gels. The gels were dried at 230 °C for more than 3 h in order to form xerogels. The nanoparticle samples were obtained after annealing the products at 350 °C, 500 °C and 700 °C in 2 h. The thermal decomposition of the gel precursor and the formation of the cubic spinel phase were monitored by DTA/TG measurements (Universal V2960T).

X-ray diffraction (Cu-Kα, Siemens D-5000) was employed to identify the crystal structure of the samples at room temperature. Transmission electron microscope (JEOL 1010) was used to examine the particle size and morphology. Thermomagnetic measurement was carried out by using a vibrating sample magnetometer (DMS) in low applied magnetic field (100 Oe) and at temperatures from 300 to 950 K. The magnetic loops in the temperature range from 5 K to room temperature were measured using a superconducting quantum interference device (SQUID) by Quantum Design with maximum field of 50 kOe.

3. Results and discussion

3.1. DTA/TG, XRD and TEM analyses

In order to investigate the formation of the xerogel from the gel, thermal analysis of the gel product was carried out. In Fig. 1 DTA curve shows the presence of two exothermic peaks. The first exothermic peak around 230 °C in DTA, accompanied with large weight loss in TG is probably due to decomposition of metal citrate precursor with simultaneous evolution of CO and CO_2 gas. The decomposition temperature range is 210–253 °C with peak temperature at 230 °C. This is corroborated by results of earlier studies on some ferrite where it has been shown that during citrate method, the first exothermic peak with large weight loss is due to decomposition of metal citrate [13–15]. The second exothermic peak at 345 °C in the DTA curve is due to formation and crystallization of the ferrite phase.

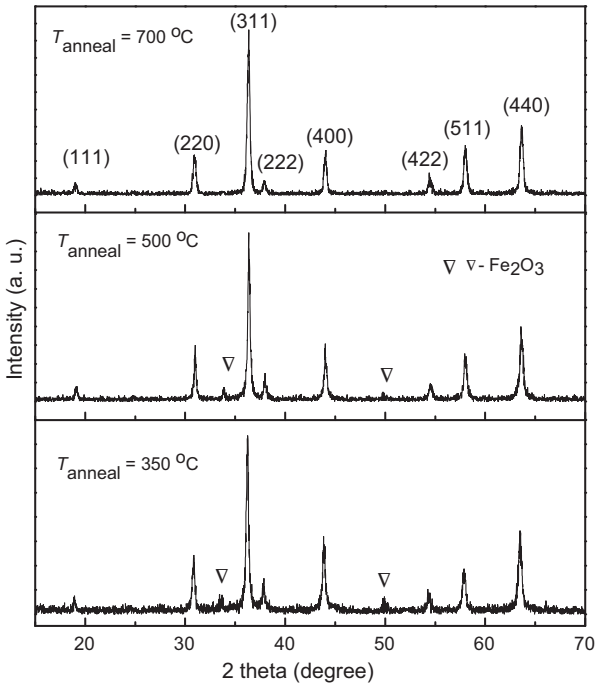

Fig. 2. Indexed XRD patters of the nanosized nickel ferrite annealed at 300 °C, 500 °C and 700 °C.

The formation of the cubic spinel oxide phase in the three samples is confirmed by the XRD patterns shown in Fig. 2. For those annealed at 350 °C and 500 °C, a small amount of impurity is observed which can be identified as α-Fe_2O_3 phase. The lattice parameters a were computed using the interplanar distance d and the respective (h,k,l) parameters. The broad XRD lines indicate that the particles are of nanosize range. The average particle size for each sample has been calculated using the Debye–Scherrer formula. The peaks of (1 1 1), (2 2 0), (3 1 1), (2 2 2), (4 0 0), (4 2 2), (5 1 1) and (4 0 0) have been deconvoluted to Lorentzian curves for the determination of the crystallite size using full-width at half-maximum value. The structural parameters are listed in Table 1. It is found that the a values of the samples are in good agreement with that reported for the bulk material (8.33 Å) [1] and the average crystallize size D_{XRD} is in the range 26.18–28.55 nm which does not change significantly with annealing temperatures.

The shape, size and morphology of the single-phase particles were examined by direct observation via transmission electron microscopy. The TEM micrographs of the sample given in Fig. 3a reveal that the particles are approximately spherical in shape and agglomerated. The particle size histogram from sampling of about 300 particles from different TEM micrographs is presented in Fig. 3b. The particle size values are distributed in a range of 21–82.5 nm. The particle size data was modeled with the lognormal distribution from that the most probable diameter D_{TEM} of 55.4 nm was deduced. A comparison between the particle sizes observed via

Table 1
Lattice constant a and mean crystallite size D_{XRD} of the nanocrystalline nickel ferrite samples annealed at 350 °C, 500 °C and 700 °C.

Annealing temperature (°C)	a (Å)	D_{XRD} (nm)
300	8.332	28.55
500	8.333	28.50
700	8.331	26.18

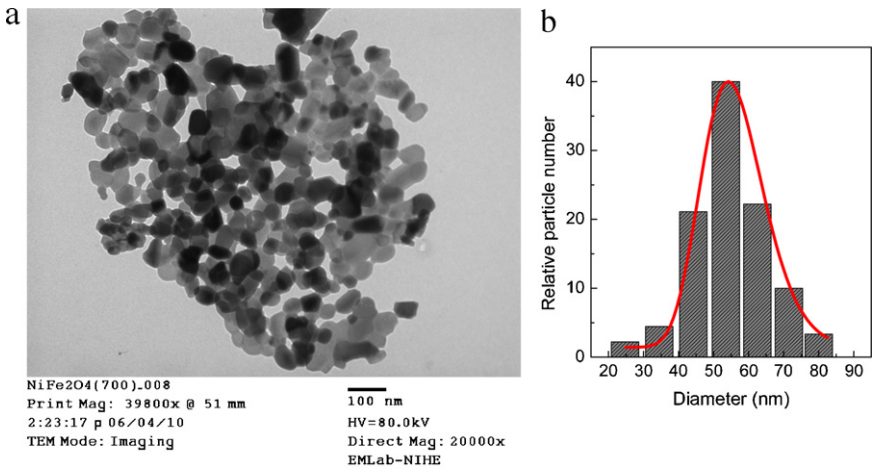

Fig. 3. (a) Transmission electron micrograph of the nanocrystalline nickel ferrite sample annealed at 700 °C. (b) Histogram of the particle size distribution obtained from sampling of nanoparticles from TEM data. The solid curve is the fit to the lognormal distribution function.

TEM and the crystallize size determined via XRD data show that the particles with broad size distribution may contain from one to a few crystallites.

3.2. Magnetization measurements

Magnetic measurements were performed in the single-phase $NiFe_2O_4$ particles which was annealed at 700 °C. The temperature dependence of the magnetization $M(T)$ in applied field $H = 100$ Oe is shown in Fig. 4. With increasing temperature, the magnetization was approximately constant until a large drop occurred beginning at 810 K which indicates a ferrimagnetic to paramagnetic transition. The Curie temperature T_C is determined as the temperature corresponding to the minimum of the dM/dT versus T curve in the temperature range above 810 K as indicated in the inset of Fig. 4. A T_C value of 873 K was found which is comparable to the value 870 K for bulk material [1]. The agreement between the Curie temperature values suggests that the cation distributions in the two crystallographic A and B sites in the studied nanoparticles are similar to that in the bulk. As already known, the Curie temperature of inverse spinel ferrites depends on the exchange interactions where the intersublattice interactions J_{AB} is stronger than the intrasublattices J_{AA} and J_{BB} with $J_{AB} \gg J_{BB} \gg J_{AA}$ [16]. For nickel ferrite, the strongest interaction is the one between Fe^{3+} in A site and Ni^{2+} in B site [9].

The magnetic isotherms $M(H)$ were made at different temperatures from 5 K to 300 K. For demonstration, the hysteresis loops at 5 K and 300 K are presented in Fig. 5. The inset of the figure shows a magnified region around the origin from that the coercivity H_c is determined. A common feature of the loops at different temperatures is that the magnetization approaches to saturation around 13 kOe and followed by a slow increase of the magnetization with further increasing magnetic field. This behavior has generally been observed in many ferrite nanoparticle systems and is a result of the formation of canted or disordered spins at the surface shell. The spontaneous magnetization M_s of the ferrimagnetic core is determined by extrapolating the high-field linear part of the magnetization curve to zero field.

The spontaneous magnetization of the sample is 46 emu/g at $T = 5$ K, corresponding to 82% of the saturation magnetization value reported for bulk material at the same temperature (56 emu/g) [1]. In the core–shell model for magnetic nanoparticles, with D the diameter of the particle, t the outer-shell thickness and assuming identical mass density in the whole particle volume, the experimental M_s and bulk M_s are related via the following expression [17]:

$$M_s^{\text{experimental}} = M_s^{\text{bulk}} \left[\frac{D/2 - t}{D/2} \right]^3 \quad (1)$$

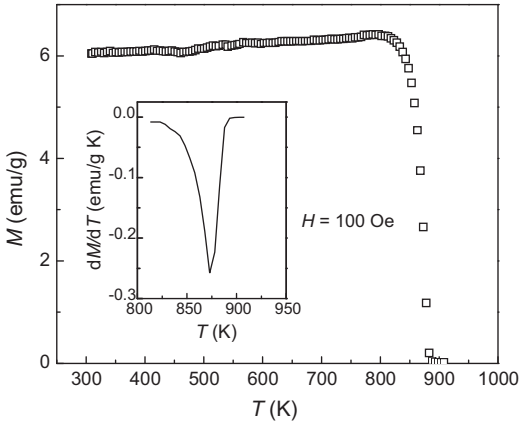

Fig. 4. Temperature dependence of magnetization in $H = 100$ Oe of the nanosized nickel ferrite annealed at 700 °C. The inset shows the dM/dT versus T curve in the magnetic transition region where the Curie temperature is determined (see text).

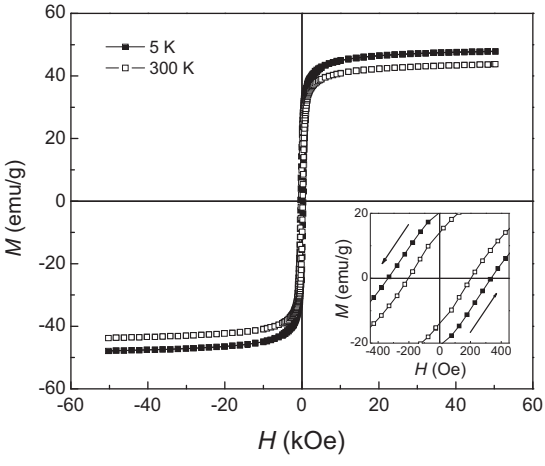

Fig. 5. Hysteresis loops measured at 5 K and 300 K up to maximum field ±60 kOe for the nanosized nickel ferrite annealed at 700 °C. The inset shows the magnified region around the origin.

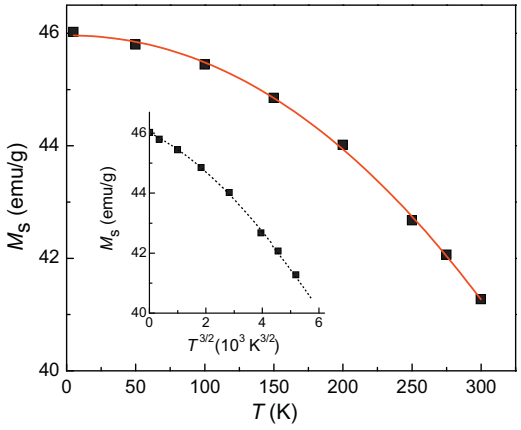

Fig. 6. Spontaneous magnetization M_s as a function of temperature for the nanosized nickel ferrite annealed at 700 °C. The solid line is the fit curve according to modified Bloch law for the saturation magnetization of ferromagnetic materials. The inset shows the spontaneous magnetization as a function of $T^{3/2}$ (dashed line is for guiding the eyes).

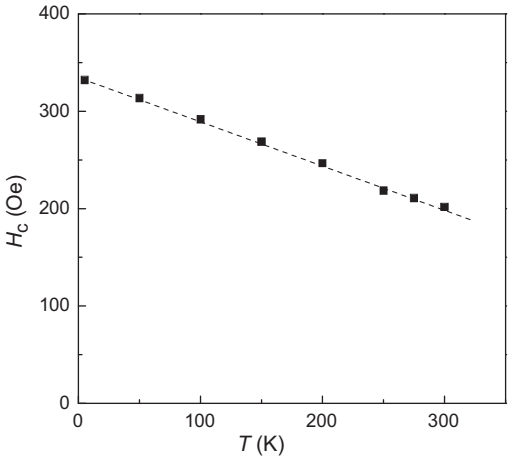

Fig. 7. Temperature dependence of coercivity H_c the nanosized nickel ferrite annealed at 700 °C.

We estimate the ratio $M_s^{experimental}/M_s^{bulk}$ for the studied nanoparticles based on Eq. (1). With t approximated by a lattice constant (8.33 Å) and particle sizes D varying from 21 nm to 82.5 nm, $M_s^{experimental}/M_s^{bulk}$ has values in the range 78–94%. The calculation indicates that the reduced spontaneous magnetization of the sample can be accounted for the canted or disorder spins in the surface shell. The M_s value also supports the fact that in this sample Ni^{2+} ions (almost) entirely locate in B sites because due to the lower spin moment of Ni^{2+} ($S = 2\ \mu_B$/ion) compared to that of Fe^{3+} ($S = 5\ \mu_B$/ion), the occupation of Ni^{2+} ions in A sites would results in an increase of the net magnetization according to the Néel configuration.

In Fig. 6, the M_s values at different temperatures are plotted. For an infinitely large ferromagnetic system, M_s below the Curie temperature (about half of T_C) follows the Bloch law [18]

$$M_s(T) = M_s(0)\left[1 - \left(\frac{T}{T_0}\right)^{\alpha}\right] \quad (2)$$

where $M_s(0)$ is the spontaneous magnetization at zero kelvin, $(1/T_0)^{\alpha}$ is the Bloch constant and T_0 is the temperature at which the spontaneous magnetization is zero. This law is generally valid for ferro- and ferrimagnetic bulk materials including ferrites [1,18] with the exponent value $\alpha = 3/2$ since the spin-wave excitation is a mechanism only available at relatively low temperature in these systems. As the size of the system is reduced to nanoscale, due to finite size effects, the thermal dependence of magnetization deviates from the Bloch law because the magnons with wavelength larger than the particle dimensions cannot be excited and a threshold of thermal energy is required to generate spin waves in these small particles. Thus for nanoparticles, the spin-wave spectrum is modified in the form of power law (T^{α}) with the Bloch exponent larger than its bulk value. This is known as the modified Bloch law reported by Hendriksen et al. for ferromagnetic clusters of various structures (bcc, fcc and amorphous) [19]. Their calculations show that finite size causes an effective T^2 dependence for the spontaneous magnetization of these systems at low temperature. Linderoth et al. [20] reported the modified Bloch's law for amorphous Fe–C ultrafine particles where the large deviation from the $T^{3/2}$ dependence is the result of several finite size effects like an energy gap in the density of states for the spin waves and lack of magnetic coordination at the surface of nanoparticles. The modified Bloch law has also been observed for magnetization of various nanosized ferrites [10,21,22]. In a recent work by Maaz et al. on the magnetic properties of the nickel ferrite nanoparticles with particle size 24 ± 4 nm prepared by coprecipitation method [10], the saturation magnetization of was found to follow the modified Bloch's law in the temperature range from 50 to 300 K with the $\alpha = 2$. Below 50 K, the magnetization increases abruptly which was attributed to the presence of freezed surface spins and possible paramagnetic impurities that are activated at low temperatures. Referring to our sample, the inset of Fig. 6 shows the spontaneous magnetization as a function of $T^{3/2}$. From this plot it is clear that the spontaneous magnetization does not decrease linearly with $T^{3/2}$. The best fit to the magnetization in the whole temperature range from 5 K to 300 K using the expression in Eq. (2) yields $M(0) = 45.96 \pm 0.04$ emu/g, $T_0 = 899.30 \pm 35.45$ K and $\alpha = 2.07 \pm 0.07$. It is noted that the deduced T_0 value is in agreement with the T_C value determined via the thermomagnetic measurement.

The coercive fields at different temperatures as calculated from $M(H)$ loops are plotted in Fig. 7. We found that H_c decreases almost linearly with increasing T in which the H_c value at $T = 300$ K is 60% of the value at $T = 5$ K. The H_c value in this particular case is influenced by various factors arising primarily from the broad particle size distribution and their temperature-dependent characteristics are difficult to be separated from one and another. According to previous works [11,12], the particle size limit below which nickel ferrite is in the single domain state is around 35 nm, our sample therefore contains both types of single and multi domain particles in which the latter has a larger volume fraction (Fig. 3). In the single domain particles, the irreversible rotation of magnetization is the only mechanism of coercivity. For noninteracting single domain magnetic particles with uniaxial anisotropy the temperature dependence of coercivity can be described in the form of simple model (Kneller's law) of thermal activation of particles' moment over the anisotropy barriers as [23]

$$H_c(T) = H_c(0)\left[1 - \left(\frac{\zeta k_B T}{KV}\right)^{1/2}\right] \quad (3)$$

in which $H_c(0)$ is the coercivity at $T = 0$ K, K is the magnetic anisotropy energy per volume and V the volume of the individual particle. The ζ is a coefficient that depends on the time required for measuring a value of magnetic order parameter. For the nickel ferrite nanoparticles studied by Maaz et al., the particle sizes (24 ± 4 nm) are well below the single domain size limit and the coercivity was found to follow Kneller's law fairly well in the temperature range from 10 K to 300 K [10]. However, large deviation from this law can occur if the volume V of the single domain particles varies in a broader range. On the other hand, for the multi

domain particles, domain magnetizations are usually reversed by the displacement of domain walls before irreversible rotation magnetization occurs. The coercivity in this case depends on the factors such as surface energy of domain wall, internal stress, voids, inclusions, etc. in the particles [24,25]. The temperature dependent behavior may be described by one or more of the terms in the expression [26]

$$H_c(T) = \frac{C_1[A(K + 3/2\lambda\sigma)]^{1/2}}{M_s} + C_2 M_s + \frac{C_3(K + 3/2\lambda\sigma)}{M_s} \quad (4)$$

where $A(T)$, $K(T)$ and $\lambda(T)$ are the exchange, anisotropy and magnetostriction constants, respectively, σ is the internal stress, and C_i are appropriate coefficients. It should be noted that apart from the above factors, the randomness of anisotropy axes and interparticle interactions may also influence the temperature dependence of coercivity in the case of nanoparticles [27,28].

4. Conclusions

Nanosized nickel ferrites were prepared by the citrate precursor method. Crystallization process was studied for different annealing temperatures. The mean crystallite size does not change significantly in the annealing temperature range. The single phase sample was obtained with annealing temperature 700 °C. TEM measurements reveal that the particle assembly has a broad size distribution. The lattice constant and Curie temperature of the sample is in agreement with those of the bulk material whereas a decrease in magnetization at $T = 5$ K was found which can be attributed to disorder or canted spins in the surface layer of the particles. At temperatures between 5 K and 300 K, the spontaneous magnetization follows the modified Bloch law for ferromagnetic materials which is due to their finite size effects. In the same temperature range, the coercive field decreases linearly with increasing temperature. Different coercivity mechanisms were discussed for this particular nanoparticle assembly.

Acknowledgments

The work was supported by Vietnam's National Foundation for Science and Technology Development (NAFOSTED) Grant No. 103.02.105.09. The authors would like to thank Prof. Kenjiro Miyano for the use of the equipment in his laboratory and Dr. Naoki Ogawa for his technical assistance.

References

[1] S. Krupička, P. Novák, in: E.P. Wohlfarth (Ed.), Ferromagnetic Materials, vol. 3, North-Holland, Amsterdam, 1982.
[2] J. Smit, H.P.J. Wijn, Ferrites, Philips Technical Library, 1959.
[3] K. Ishino, Y. Narumiya, Ceram. Bull. 66 (1987) 1469.
[4] A. Goldman, Modern Ferrite Technology, 2nd edition, Springer Science, 2006.
[5] J.L. Dormann, D. Fiorani, Magnetic Properties of Fine Particles, North-Holland, Amsterdam, 1992.
[6] I. Safarik, M. Safarikova, Monatshefte für Chemie 133, Springer-Verlag, 2002, pp. 737–759.
[7] A. Kale, S. Gubbala, R.D.K. Misra, J. Magn. Magn. Mater. 277 (2004) 350–358.
[8] E.C. Sousa, M.H. Sousa, H.R. Rechenberg, G.F. Goya, F.A. Tourinho, R. Perzynski, J. Depeyrot, J. Magn. Magn. Mater. 310 (2007) e1020–e1022.
[9] R.H. Kodama, A.E. Berkowitz, E.J. McNiff, S. Goner, Phys. Rev. Lett. 77 (1996) 394(4).
[10] K. Maaz, A. Mumtaz, S.K. Hasanain, M.F. Bertino, J. Magn. Magn. Mater. 322 (2010) 2199–2202.
[11] R. Malik, S. Annapoorni, S. Lamba, V.R. Reddy, A. Gupta, P. Sharma, A. Inoue, J. Magn. Magn. Mater. 322 (2010) 3742–3747.
[12] S. Singhal, J. Singh, S.K. Barthwal, K. Chandra, J. Solid State Chem. 178 (2005) 3183–3189.
[13] S. Dey, A. Roy, D. Das, J. Ghose, J. Magn. Magn. Mater. 270 (2004) 224–229.
[14] V.K. Sankaranarayanan, Q.A. Pankhusrt, D.P.E. Dickson, C.E. Johnson, J. Magn. Magn. Mater. 130 (1994) 288–292.
[15] S. Prasad, N.S. Gajbhiye, J. Alloys Compd. 265 (1998) 87–92.
[16] A. Broese van Groenou, P.F. Bonger, A.L. Stuyts, Mater. Sci. Eng. 3 (1968–1969) 317–392.
[17] K. Parekh, R.V. Upadhyay, L. Belova, K.V. Rao, Nanotechnology 17 (2006) 5970.
[18] F. Bloch, Z. Phys. 61 (1931) 206–219.
[19] P.V. Hendriksen, S. Linderoth, P.-A. Lindgård, J. Magn. Magn. Mater. 104–107 (1992) 1577–1579.
[20] S. Linderoth, L. Balcells, A. Labarta, J. Tejada, P.V. Hendriksen, S.A. Sethi, J. Magn. Magn. Mater. 124 (1993) 269–276.
[21] J.P. Chen, C.M. Sorensen, K.J. Klabunde, G.C. Hadjipanayis, E. Devlin, A. Kostikas, Phys. Rev. B 54 (1996) 9288(9).
[22] C.R. Alves, R. Aquino, M.H. Sousa, H.R. Rechenberg, G.F. Goya, F.A. Tourinho, J. Depeyrot, J. Met. Nanocryst. Mater. 20–21 (2004) 694–699.
[23] C.P. Bean, J.D. Livingston, J. Appl. Phys. 30 (1959) S120(10).
[24] J.B. Goodenough, Phys. Rev. 95 (1954) 917–932.
[25] S. Chikazumi, Physics of Magnetism, Wiley, New York, 1964, pp. 281–391.
[26] F.C. Schwerer, C.E. Spangler Jr., J.F. Kelly, Acta Metall. 26 (1978) 579–589.
[27] W. Luo, S.R. Nagel, T.F. Rosenbaum, R.E. Rosensweig, Phys. Rev. Lett. 67 (1991) 2721(4).
[28] R. Malik, S. Annapoorni, S. Lamba, P. Sharma, A. Inoue, J. Appl. Phys. 104 (2008) 064317(7).